

# Improving the quality of phase maps in phase object digital holographic interferometry by finding the right reconstruction distance

Eva-Lena Johansson,\* Lars Benckert, and Mikael Sjö Dahl

Division of Experimental Mechanics, Luleå University of Technology, SE-971 87 Luleå, Sweden

\*Corresponding author: eva-lena.johansson@ltu.se

Received 21 June 2007; revised 16 October 2007; accepted 27 October 2007;  
posted 31 October 2007 (Doc. ID 84360); published 20 December 2007

Improved quality of phase maps in pulsed digital holographic interferometry is demonstrated by finding the right reconstruction distance. The objective is to improve the optical phase information when the object under study is a phase object and when it is out of focus, leading to low contrast fringes in the phase map. A numerical refocusing is performed by introducing an ideal lens as a multiplication by a phase field in the Fourier domain, and then a region of maximum speckle correlation is found by comparing undisturbed and disturbed subimages in different refocused imaging planes. After finding the right reconstruction distance, a phase map of high visibility is constructed. By this technique a 30% reduction of the phase error for a flow of helium gas and a 50% reduction of the phase error for a weak thin lens were obtained, which resulted in a significant improvement of the visual appearance of the phase maps. © 2008 Optical Society of America

OCIS codes: 090.2880, 090.1995, 120.6150.

## 1. Introduction

Pulsed holographic interferometry [1], or the all-electronic version pulsed TV holography, is a method used to study the change of an object between two specific instants of time. The method is sensitive to the accumulated optical path length difference between the two object states acquired. Hence the phase difference between two points along the propagation direction of a plane wave is equal to the optical path length difference multiplied by the wave-number. The deformation of a solid object or the refractive index change along the light path, caused by a phase object, may be measured. Following Goodman [2] the phase error in the reconstruction, and hence the quality of the reconstructed phase map, strongly depends on the speckle correlation between the two reconstructed fields. Having a high-quality phase map improves the reliability of the measurement and simplifies further processing of the result, for example phase unwrapping. It is therefore desirable trying to optimize the speckle correlation be-

tween the two recordings prior to phase unwrapping, either through a good choice of experimental settings based on *a priori* knowledge about the measurement outcome or through postprocessing of the two acquired speckle fields before calculating the phase map.

The holographic interferometry (or TV holography) technique is known to be limited to situations where small object deformations are present. The reason is that high-quality fringes only can be produced in points where there is a significant overlap, and hence high correlation, between the speckles in the two reconstructions. In the case when a phase object is placed in a laser speckle field, large speckle displacements may be present compared to the situation when no object is present. The phase quality may therefore be poor. This problem was addressed by Andersson *et al.* [3] and Molin *et al.* [4] a few years ago. Their solution was to calculate the speckle displacement field in the image plane between the two recordings using digital speckle photography and form the phase maps between the two fields based on the outcome of that calculation. Hence the phases in different pixels in the two recordings are in general compared. With this technique the authors have shown that high-quality phase maps may be con-

structed despite the presence of a large bulk or rotating motion of the object. A well-known effect in holographic interferometry is that the fringes do not necessarily localize on the surface of the test object [5,6]. A pivot motion, which is the rotation of an object surface about an axis parallel to its surface, will generate fringes that lie very near the object surface. For in-plane rotation, the fringes will be localized in the region of a line in space, normal to the object surface. An in-plane translation may not produce any fringes on the object surface, but at the back focal plane of a lens, i.e., the fringes are localized at infinity. Following Yamaguchi the reason is that the fringes localize on a surface in three-dimensional space of zero speckle movement, and hence maximum speckle correlation between the two reconstructions [7]. This is the same surface where the phase maps ideally should be constructed in order to have the best possible quality. Because of the much lower numerical apertures involved in the construction of digital holograms, and as a result long speckles along the optical axis, the concept of fringe localization in TV holography is seldom acknowledged. To get phase maps of the best possible quality, however, the surface of best speckle correlation between the two recordings should be identified before constructing the phase map. Having the optical fields stored as digital holograms, one way to find this surface is using the possibility to refocus the images by the concept of digital holography.

The concept of digital holography has evolved quite rapidly during the past decade, with one of its main features being the possibility to control the reconstruction distance numerically [8,9]. In 1992 Haddad *et al.* [10] described a holographic microscope based on numerical reconstruction of Fourier-transform holograms and recently a method was proposed for automatic focus tracking during the recording of a sequence of holograms while the sample experiences axial displacement [11]. Controlling the pixel pitch of the reconstruction independently of wavelength and reconstruction distance is a problem typical of digital holography and a problem that recently has been addressed by several researchers [12,13]. The objective of this paper is to investigate a method to refocus digital image plane holograms with the objective to improve the quality of the optical phase information between two recordings when the object under study is a phase object. We will also show a method to find maximum contrast in the phase map. In contrast to the combined method of Andersson *et al.* [3] for a phase object, finding the surface of maximum correlation will directly give additional information about the position and extension of the phase object as well as a high-quality phase map. The experimental setup used in the investigation is outlined in Section 2 and the theoretical considerations of the technique are described in Section 3 of the paper. The experimental results are presented in Section 4 and discussed in Section 5. The paper finishes with a few concluding remarks.

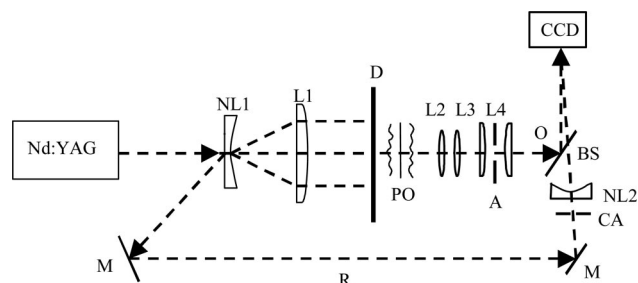


Fig. 1. Experimental setup. Nd:YAG, pulsed laser; CCD, CCD camera; M, mirror; NL1 and NL2, negative lenses; L1, collimation lens; L2–L4, lens system for imaging; D, diffuser; PO, phase object; A, quadratic aperture; CA, circular aperture; BS, beam splitter; O, object beam; R, reference beam.

## 2. Experimental Setup

An experimental setup for the pulsed TV holography system is shown in Fig. 1. An injection-seeded, twin cavity, pulsed, and frequency doubled Nd:YAG laser (Spectron SL804T) is used as the light source. For the green light (wavelength  $\lambda = 532$  nm) it has a maximum pulse energy of 200 mJ/pulse at a repetition rate of 10 Hz. The pulse duration is  $\sim 13$  ns, which makes it possible to study transient phase objects. Light from the Nd:YAG laser is expanded by a plano-concave lens NL1 and lens L1 collimates the light. The phase object, PO, under study is placed in front of a diffuser, which is imaged on the detector by lenses L2–L4. Lens L2 is an achromatic doublet and it has a focal length of 100 mm, lens L3 is biconvex and it has a focal length of 30 mm and lenses L4 have a focal length of 100 mm for each plano-convex lens. The magnification of the total system is 0.33. A detailed sketch of the imaging system is shown in Fig. 2 where the exit pupil of the system is also indicated. The detector is a CCD camera, PCO Sensicam double shutter, with a resolution of  $1280 \times 1024$  pixels, a pixel size of  $6.7 \times 6.7 \mu\text{m}^2$  and a dynamic range of 12 bits. The camera is computer controlled via a fiber optic cable and it is externally triggered. A quadratic aperture A, with a size of  $2 \text{ mm} \times 2 \text{ mm}$ , in the imaging system reduces the spatial frequencies to be resolved by the detector. A small portion of light is reflected at the plane surface of NL1 and is used as

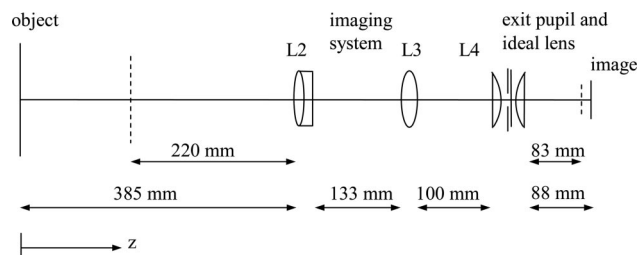


Fig. 2. Configuration used for the calculation in ZEMAX. The ideal lens is put in the exit pupil plane. When the object plane is chosen closer to the imaging system (a dashed line), the focal length of the ideal lens has to be chosen to maintain a constant magnification and as a consequence the image plane is moved closer to the imaging system (a dashed line).

reference beam R. The reference beam passes a negative lens NL2 spreading the light uniformly onto the detector. As seen from the detector, the reference beam is adjusted so that its virtual image (a bright spot) is located one slit width from the edge of the aperture. This angular offset between the object and the reference beams separates the interference terms, between the object beam O and the reference beam (OR\* and O\*R, respectively, where \* denotes complex conjugate), from the self-interference of the light (RR\* and OO\*) passing the aperture in the Fourier domain. One of these cross spectra (OR\* or O\*R) may be filtered out, moved to the low-frequency domain, and transformed back to the image plane. The complex amplitude thus obtained represents a scaled replica of the original complex amplitude of the object field at the image plane of the system. The technique is thoroughly described by Schedin and Gren [14].

### 3. Method

The objective of this paper is to find the surface in three-dimensional space between the diffuser and the first lens having the highest speckle correlation between the two recordings and to construct the phase map in that plane. First we need a technique to refocus the image numerically. The technique we have chosen for this research is based on the simple Fourier-transform relation between the exit pupil of an imaging system and its image plane [15]. In essence we make a Fourier transform of the complex amplitude in the image plane; multiply by the phase term

$$U(\xi, \eta) = \exp(-ik\sqrt{f^2 + \xi^2 + \eta^2}) \quad (1)$$

for an ideal thin lens, where  $f$  is the focal length of the lens,  $\xi$  and  $\eta$  are spatial frequency coordinates, and  $k$  is the wavenumber; and then transform back to the new image plane. As a further criterion we have chosen to keep the magnification constant during the reimaging. Two design questions arise with this technique. The first question is which focal length to use for the numerical lens for a given refocusing distance and the second question is which reconstruction distance that particular choice of lens results in when the spectra are transformed back to the new image plane. Since these questions are nontrivial for a general imaging system we have used the design program ZEMAX to answer these questions for the specific setup in Fig. 2. The result is seen in Fig. 3. Choosing the numerical lens indicated in Fig. 3 for a given refocusing distance will result in a new image with the same magnification as the original image. The problem is that it will be represented on a grid with a pitch given by

$$\Delta x_{i2} = \Delta x_{i1} \frac{z_2}{z_1}, \quad (2)$$

where index 1 refers to the original position, relative to the exit pupil, and pixel size of the detector; and index 2 refers to the new reconstructed position and

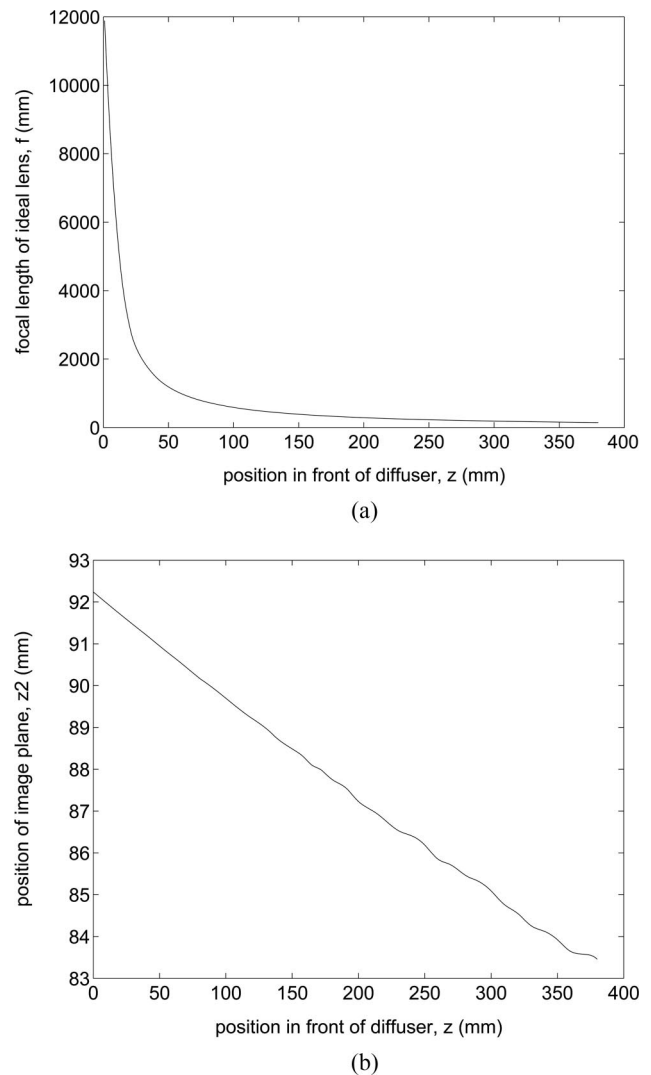


Fig. 3. (a) Calibration curve for the numerical lens to use in the exit pupil of Fig. 2. (b) The reimaging distance as a function of refocus distance. These curves are obtained from ZEMAX by optimizing for a constant magnification for a given refocus distance.

pixel size of the detector. As the virtual detector moves towards the imaging system the pixels hence become smaller. As an example a reimaging of 165 mm is indicated in Fig. 2. The focal length of the numerical lens to use in this case becomes 351 mm, which results in a change in pixel size from 6.7 to 6.4  $\mu\text{m}$ . To simplify further processing all image planes are resampled on a common grid.

Using the technique described above, the speckle fields before and after a change in the phase object has been introduced can be constructed for a general imaging plane. Calculating the correlation coefficient  $\gamma$  defined as

$$\gamma = \frac{\sum_i^P \sum_j^P (I_1(i, j) - \bar{I}_1)(I_2(i, j) - \bar{I}_2)}{\left\{ \left[ \sum_i^P \sum_j^P (I_1(i, j) - \bar{I}_1)^2 \right] \left[ \sum_i^P \sum_j^P (I_2(i, j) - \bar{I}_2)^2 \right] \right\}^{1/2}} \quad (3)$$

between these two speckle patterns gives a measure of the relative overlap between the two speckle fields and hence the possibility to construct a high-quality phase map in that plane. In Eq. (3)  $I_1$  and  $I_2$  are the speckle intensities in the images, before and after a change in the phase object, respectively. The pixel positions within the correlation window of size  $p^2$  pixels squared are denoted by  $i$  and  $j$ , and the mean intensities of images  $I_1$  and  $I_2$  are denoted by  $\bar{I}_1$  and  $\bar{I}_2$ , respectively. Locating the plane of maximum correlation along the optical axis hence gives the plane in which the phase map should be constructed in order to be of the highest possible quality. Once this plane is located a wrapped phase map is constructed in the usual manner using the formula [14]

$$\Delta\phi = \arctan\left[\frac{\text{Re}(s)\text{Im}(s') - \text{Im}(s)\text{Re}(s')}{\text{Im}(s)\text{Im}(s') + \text{Re}(s)\text{Re}(s')}\right], \quad (4)$$

where  $s$  and  $s'$  are the complex amplitudes of the speckle fields at the two object states. Convolution with a  $3 \times 3$  kernel is used to smooth the data prior to calculating the phase.

#### 4. Results

Two different experiments are performed to verify the method. In the first experiment, a flow of helium gas is used as a phase object and in the second experiment, a thin spherical lens is used.

##### A. Phase Object Is a Flow of Helium Gas

An experiment is performed where the phase object is a flow of helium gas. The center of a circular gas nozzle with a 4 mm diameter is placed 165 mm in front of the diffuser, according to the experimental setup in Fig. 1. The velocity of the gas at the opening of the nozzle is 6 m/s, measured with a flow meter. Images before and after the gas flow has been turned

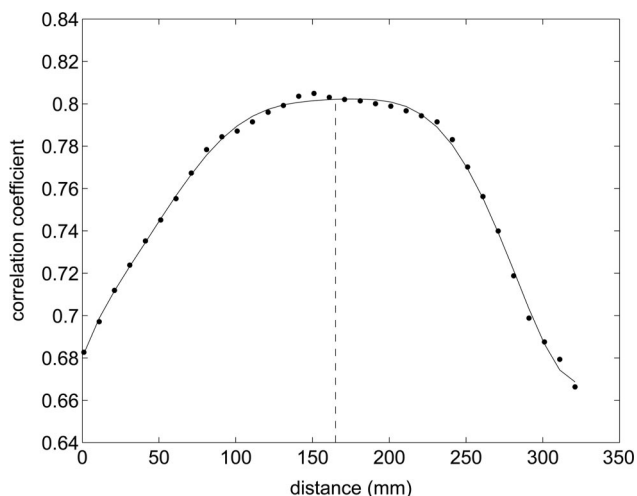


Fig. 4. Correlation coefficient versus distance from the diffuser for subimage pairs, without and with the helium gas present. The dashed line represents the distance 165 mm, which is in the middle of the gas nozzle.

on are reconstructed in the plane of the diffuser and at every tenth millimeter in front of it to a distance of 320 mm. A series of subimages ( $128 \times 128$  pixels) are correlated according to Eq. (3) for the different imaging planes. The resulting correlation coefficients are plotted versus distance in front of the diffuser in Fig. 4 for subimages situated in the middle of the images. Maximum correlation is found at a distance 150 mm

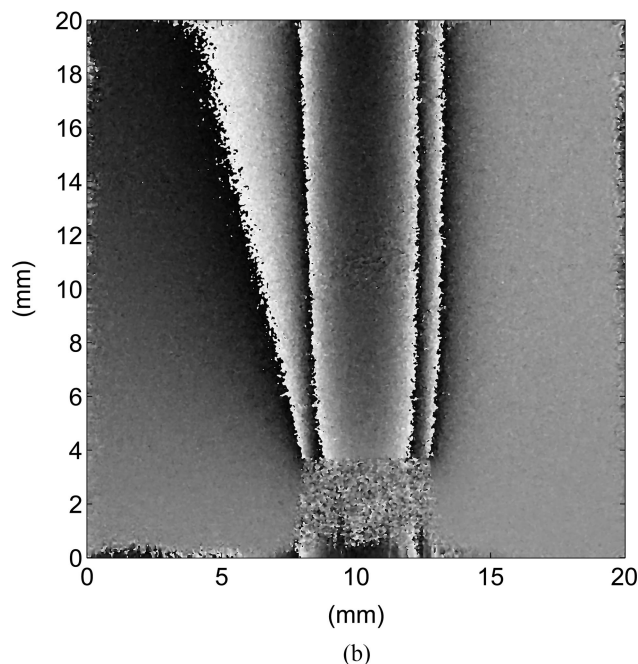
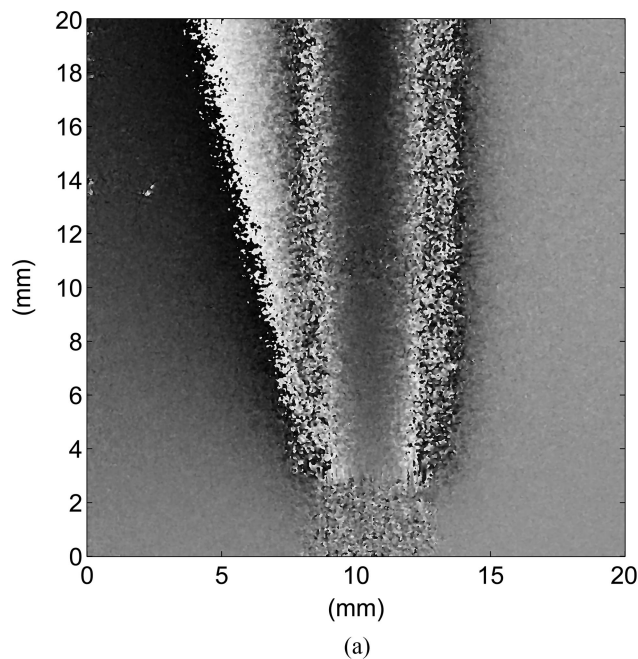


Fig. 5. Wrapped phase maps obtained from a flow of helium gas surrounded by air and placed 165 mm in front of a diffuser. The flow enters from below. (a) Wrapped phase map obtained from the plane of the diffuser. Low contrast fringes are seen. (b) Wrapped phase map obtained from a plane in the middle of the gas after numerical refocusing. High contrast fringes are seen.

in front of the diffuser. For the whole image the position of maximum correlation is determined to  $166 \pm 10$  mm (mean value  $\pm$  standard deviation) in front of the diffuser.

The phase map obtained when the image is focused on the diffuser is compared to the phase map obtained when the numerical refocusing technique has been used to focus in the plane of maximum speckle correlation. The phase maps are seen in Figs. 5(a) and 5(b). The phase map obtained from the plane of the diffuser is visually of lower quality because of speckle displacements as compared to the phase map obtained from the plane in the middle of the gas.

#### B. Phase Object is a Spherical Lens

An experiment is performed where the phase object is a thin spherical lens. The 75 mm diameter lens is meniscus shaped with power of +0.25 diopters and a center thickness of 2.15 mm. From its meniscus shape and its refractive index of 1.525 we conclude that its principal planes are positioned 27 mm outside the lens. The lens is placed with its principal planes 78 mm in front of the diffuser, according to the experimental setup in Fig. 1. A series of subimages ( $128 \times 128$  pixels) are correlated according to Eq. (3) after numerical refocusing to different imaging planes as before. The images are again reconstructed in the plane of the diffuser and at every tenth millimeter in front of it to a distance of 190 mm. The resulting correlation coefficients are plotted versus distance in front of the diffuser in Fig. 6 for a case where the subimages are situated in the middle of the images. This time the maximum correlation is found at a distance 80–90 mm in front of the diffuser. The dashed line shows the position of the principal planes of the lens. For the whole image the position of maximum correlation is determined to  $78 \pm 17$  mm (mean value  $\pm$  standard deviation) in front of the diffuser.

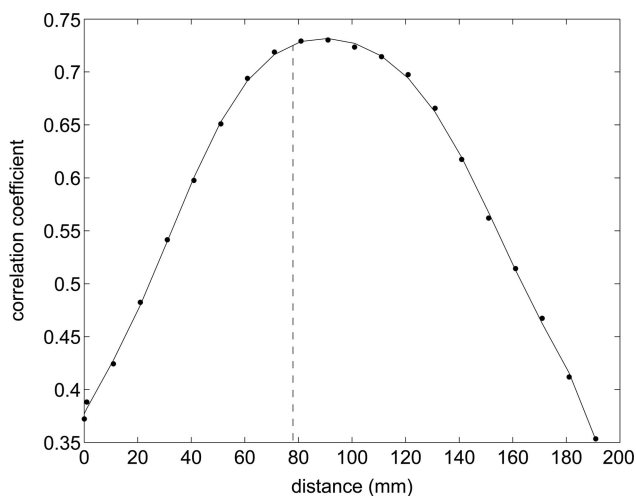


Fig. 6. Correlation coefficient versus distance from the diffuser for subimage pairs, without and with the thin lens present. The dashed line represents the distance 78 mm, which is the localization of the principal planes of the thin lens.

The phase map obtained when the image is focused on the diffuser is compared to the phase map obtained when the numerical refocusing technique has been used to focus at the principal planes, 78 mm in front of the diffuser. The phase maps are seen in Figs. 7(a) and 7(b). Once again the phase map obtained from the plane of the diffuser is of low quality because of speckle displacements as compared to the phase

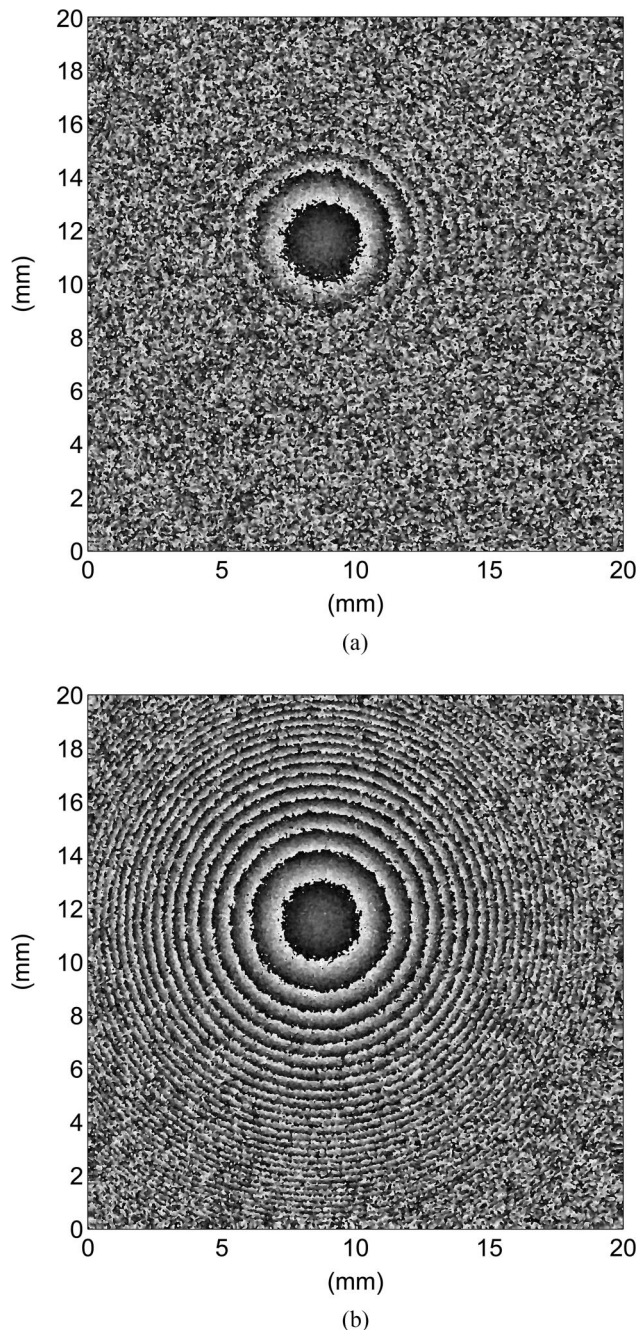


Fig. 7. Wrapped phase maps obtained from a thin lens as a phase object and placed with its principal planes 78 mm in front of a diffuser. (a) Wrapped phase map obtained from the plane of the diffuser. Low contrast fringes are seen. (b) Wrapped phase map obtained by refocusing at the principal planes of the lens. High contrast fringes are seen.

map obtained after refocusing at the principal planes of the lens.

## 5. Discussion

The numerical reimaging technique used in this paper appears to work well for the optical system and the refocusing distances used in this paper. The main attraction with the technique is its simplicity where only numerical Fourier transforms and multiplications are present. As long as the curvature of the

improvement is thus almost 30% for the helium gas and almost 50% for the lens, which results in a significant visual improvement of the phase maps.

The last point of considerable interest concerns the dynamics of the speckles caused by the change in the phase object. Because both the laser and the diffuser can be assumed stationary between the two recordings all decorrelation introduced is caused by speckle motion. The governing equation for the speckle correlation,  $\gamma$ , is written [4]

$$\gamma(\mathbf{q}) = \frac{\int_{-\infty}^{\infty} P(\mathbf{b})P^*(\mathbf{b} + \mathbf{A}_p)\exp\left[\frac{ik}{L}\mathbf{b}(\mathbf{q} - \mathbf{A})\right]\exp\left[\frac{ik}{2L^2}|\mathbf{b}|^2(\alpha - A_z)d^2\mathbf{b}\right]}{\int_{-\infty}^{\infty} |P(\mathbf{b})|^2d^2\mathbf{b}} \quad (6)$$

numerical lens is resolved the technique is also numerically stable and does not require additional padding of the matrices. As seen in Fig. 3, the focal length of the numerical lens required for a given refocusing distance becomes strongly nonlinear while the change in the position of the new image plane is essentially linear. The nonlinear relation for the focal length is expected to make the refocusing technique more prone to errors for larger refocusing distances as compared to short distances. This effect can also be seen in Fig. 3 where the value for  $z_2$  obtained from ZEMAX appears to have a larger random error for refocusing distances over 150 mm. This is also the region in which the curve for the numerical focal length becomes essentially flat.

The standard deviation of the overall phase error,  $\sigma_{\Delta\phi}$ , in a speckle interferometer was derived by Donati and Martini almost 30 years ago [16]. The expression reads

$$\sigma_{\Delta\phi} = \sqrt{\frac{\pi^2}{3} - \pi \arcsin|\mu| + \arcsin^2|\mu| - \frac{1}{2} \sum_{n=1}^{\infty} \frac{\mu^{2n}}{n^2}}, \quad (5)$$

but may be approximated by  $(\pi/\sqrt{3})(1 - |\mu|)^{0.42}$  where  $|\mu|^2 = \gamma$ . In this research the speckle correlation coefficient,  $\gamma$ , is given experimentally through Eq. (3). Using Eq. (5) the decrease in overall phase error obtained in the two experiments in this paper can be estimated. For the phase maps shown in Figs. 5 and 7, respectively, the results are an improvement from 0.88 to 0.69 rad for the flow of helium gas and from 1.22 to 0.82 rad for the lens, which should be compared with the phase error 1.81  $(\pi/\sqrt{3})$  rad between two completely uncorrelated speckle patterns. The

In Eq. (6)  $k$  is the wavenumber;  $\mathbf{q}$  is the three-dimensional correlation parameter;  $P$  is the pupil function;  $\mathbf{b}$  is a pupil plane coordinate;  $\mathbf{A}_p$  and  $\mathbf{A}$  are speckle displacements in the pupil plane and in image space, respectively; and  $L$  is the distance from the exit pupil plane to the imaging detector. Further,  $\alpha$  and  $A_z$  are components of  $\mathbf{q}$  and  $\mathbf{A}$ , respectively, along the optical axis. The first term in the numerator describes decorrelation due to speckle movements across the aperture. The first and second exponential terms are related to decorrelations due to in-plane and out-of-plane speckle displacements in image space, respectively. The essence of the technique introduced by Andersson *et al.* [3] and Molin *et al.* [4] is to search for the  $\mathbf{q}$  that maximizes Eq. (6) and to construct the phase map between those pixels. In this research instead we locate the imaging plane with zero speckle movement and construct the phase map in that plane. The effect on the quality of the phase map thus obtained will be the same. The physical significance of the current technique, however, can be acknowledged by considering the movement of speckles caused by the introduction of a phase object. Approximating the phase object with a thin phase screen  $\phi(\mathbf{r})$  where  $\mathbf{r}$  is a coordinate in the phase screen, an expression for the speckle movement is given by [17,18]

$$\mathbf{A} = -\frac{mL'}{k} \frac{\partial\phi}{\partial\mathbf{r}}, \quad (7)$$

where  $m$  is the magnification factor;  $k$  is the wavenumber;  $L'$  is the amount of defocus relative to the object, i.e., the position of the imaging plane relative to the phase object plane; and  $\partial\phi/\partial\mathbf{r}$  is the gradient

field of the phase object (in essence the gradient of the refractive index field). According to Eq. (7) there are two ways to make the speckles stationary in the imaging plane. If there are no phase gradients present  $\partial\phi/\partial\mathbf{r}$  vanishes and then obviously the speckles will remain stationary. The second way to make the speckles stationary is to focus in the plane of the phase screen. By locating the plane of maximum correlation the position of the phase object is therefore also then located. The technique described in this paper hence gives high-quality quantitative information about the average change in refractive index along the imaging direction as well as quantitative information about the position of the phase field. This technique is hence an alternative to the two techniques presented in [17] and [18] for determining the strength and position of an unknown phase object. The same conclusion about the localization of maximum speckle correlation in the plane of the phase screen can be deduced from the traditional theory of fringe localization in holographic interferometry [19]. According to that theory the fringes localize in a plane in which the phase gradients within the imaging cone become smallest. The cross-sectional area of this cone is smallest in the focus plane and hence imaging in this plane will maximize speckle correlation, and that is where the fringes are expected to localize. As seen in the optimized phase maps in Figs. 5(b) and 7(b) there are still significant amounts of phase error present, in particular in the case of the lens. The reason for this is the first term in the integrand of Eq. (6). A movement of the speckle field across the entrance pupil of the lens system will cause new independent speckles to enter the imaging system and thus cause decorrelation. According to Eq. (7) this movement is tuned by the distance between the phase screen and the entrance pupil of the imaging system. This effect cannot be corrected for with the present technique and is the reason for the remaining phase error.

## 6. Conclusions

A change in a phase object that is out of focus in a laser speckle field may give large speckle displacements. This is a problem when trying to obtain a high-quality phase map. We have shown that it is possible to change a phase map of low quality to a phase map of high quality by use of digital holography that has the properties of numerical refocusing. The exit pupil of the imaging system and the detector are treated as a Fourier-transform pair. To refocus a complex field to another imaging plane, the curvature of the field in the exit pupil is changed by multiplying the existing field by a phase field, an ideal lens of a certain focal length that is determined by an optical design program. When using this refocusing technique the magnification is kept constant. The localization of maximum speckle correlation is then found by comparing undisturbed and disturbed subimages in different imaging planes. Different refocused imaging planes give a variation of the correlation coef-

ficient, which has a maximum value at the position of smallest speckle movements. At this position the wrapped phase map is constructed. In the case of a flow of helium gas, maximum correlation occurs in a region around the center of the gas, where the speckle displacements are small. The region of localization is quite broad in this case, because of a slow variation of the phase gradients. In this experiment a reduction of the phase error in the phase map by almost 30% was obtained. In the case of a thin lens, maximum correlation occurs in a region around the principal planes of the lens. Even here the region of fringe localization is broad. For this experiment a reduction in the phase error by almost 50% was obtained and hence there was a significant improvement of the visual appearance of the phase map. The described measurement technique is applicable on different kinds of transparent media.

This research project is supported by The Swedish Research Council. The system for pulsed TV holography including the pulsed Nd:YAG laser and auxiliary equipment has been financed by the Knut and Alice Wallenberg Foundation. The authors thank Dr. Per Gren for his help with the experimental work.

## References

1. T. Kreis, *Holographic Interferometry, Principles and Methods* (Akademie Verlag, 1996).
2. J. W. Goodman, "Statistical properties of laser speckle patterns," in *Laser Speckle and Related Phenomena*, J. C. Dainty, ed. (Springer-Verlag, 1975), pp. 9–75.
3. A. Andersson, A. Runnemalm, and M. Sjö Dahl, "Digital speckle-pattern interferometry: fringe retrieval for large in-plane deformations with digital speckle photography," *Appl. Opt.* **38**, 5408–5412 (1999).
4. N.-E. Molin, M. Sjö Dahl, P. Gren, and A. Svanbro, "Speckle photography combined with speckle interferometry," *Opt. Lasers Eng.* **41**, 673–686 (2004).
5. N.-E. Molin and K. A. Stetson, "Measurement of fringe loci and localization in hologram interferometry for pivot motion, in-plane rotation, and in-plane translation, Part I," *Optik* **31**, 157–177 (1970).
6. N.-E. Molin and K. A. Stetson, "Measurement of fringe loci and localization in hologram interferometry for pivot motion, in-plane rotation, and in-plane translation, Part II," *Optik* **31**, 281–291 (1970).
7. I. Yamaguchi, "Fringe formations in deformation and vibration measurements using laser light," in *Progress in Optics*, E. Wolf, ed. (Elsevier Science, 1985), Vol. XXII.
8. U. Schnars and W. P. O. Jüptner, "Digital recording and numerical reconstruction of holograms," *Meas. Sci. Technol.* **13**, R85–R101 (2002).
9. L. Yaroslavsky, *Digital Holography and Digital Image Processing, Principles, Methods, Algorithms* (Kluwer Academic, 2004).
10. W. S. Haddad, D. Cullen, J. C. Solem, J. W. Longworth, A. McPherson, K. Boyer, and C. K. Rhodes, "Fourier-transform holographic microscope," *Appl. Opt.* **31**, 4973–4978 (1992).
11. P. Ferraro, G. Coppola, S. De Nicola, A. Finizio, and G. Pierattini, "Digital holographic microscope with automatic focus tracking by detecting sample displacement in real time," *Opt. Lett.* **28**, 1257–1259 (2003).
12. P. Ferraro, S. De Nicola, G. Coppola, A. Finizio, D. Alfieri, and G. Pierattini, "Controlling image size as a function of distance and wavelength in Fresnel-transform reconstruction of digital holograms," *Opt. Lett.* **29**, 854–856 (2004).

13. F. Zhang, I. Yamaguchi, and L. P. Yaroslavsky, "Algorithm for reconstruction of digital holograms with adjustable magnification," *Opt. Lett.* **29**, 1668–1670 (2004).
14. S. Schedin and P. Gren, "Phase evaluation and speckle averaging in pulsed television holography," *Appl. Opt.* **36**, 3941–3947 (1997).
15. J. W. Goodman, *Introduction to Fourier Optics*, 2nd ed. (McGraw-Hill, 1996).
16. S. Donati and G. Martini, "Speckle pattern intensity and phase: second-order conditional statistics," *J. Opt. Soc. Am.* **69**, 1690–1694 (1979).
17. E.-L. Johansson, L. Benckert, and M. Sjödal, "Phase object data obtained from defocused laser speckle displacement," *Appl. Opt.* **43**, 3229–3234 (2004).
18. E.-L. Johansson, L. Benckert, and M. Sjödal, "Phase object data obtained by pulsed TV holography and defocused laser speckle displacement," *Appl. Opt.* **43**, 3235–3240 (2004).
19. K. J. Gåsvik, *Optical Metrology*, 2nd ed. (Wiley, 1995).